

---

# REINFORCEMENT LEARNING IN TIME-VARYING SYSTEMS: AN EMPIRICAL STUDY

---

Pouya Hamadani<sup>1</sup> Malte Schwarzkopf<sup>2</sup> Siddhartha Sen<sup>3</sup> Mohammad Alizadeh<sup>1</sup>

## ABSTRACT

Recent research has turned to Reinforcement Learning (RL) to solve challenging decision problems, as an alternative to hand-tuned heuristics. RL can learn good policies without the need for modeling the environment’s dynamics. Despite this promise, RL remains an impractical solution for many real-world systems problems. A particularly challenging case occurs when the environment changes over time, i.e. it exhibits *non-stationarity*. In this work, we characterize the challenges introduced by non-stationarity and develop a framework for addressing them to train RL agents in live systems. Such agents must explore and learn new environments, without hurting the system’s performance, and remember them over time. To this end, our framework (1) identifies different environments encountered by the live system, (2) explores and trains a separate expert policy for each environment, and (3) employs safeguards to protect the system’s performance. We apply our framework to two systems problems: straggler mitigation and adaptive video streaming, and evaluate it against a variety of alternative approaches using real-world and synthetic data. We show that each component of our framework is necessary to cope with non-stationarity.

## 1 INTRODUCTION

— *The only constant is change. (Heraclitus 500 B.C.)*

Deep reinforcement learning has been proposed as a powerful solution to complex decision making problems (Mnih et al., 2013; Silver et al., 2018). In systems, it has recently been applied to a wide variety of tasks, such as adaptive video streaming (Mao et al., 2017), congestion control (Jay et al., 2019), query optimization (Krishnan et al., 2019; Marcus et al., 2019), scheduling (Mao et al., 2019c), resource management (Mao et al., 2016), device placement (Gao et al., 2018), and others. Reinforcement learning is particularly well-suited to these problems due to the abundance of data and its ability to automatically learn a good policy in the face of complex dynamics and objectives.

Fundamentally, reinforcement learning trains an agent by giving it feedback for decisions it makes while interacting with an environment. This interaction can occur in a controlled environment, such as a simulation or testbed, or in a real environment, such as a live deployment. While using a controlled environment seems like an attractive choice—e.g., it is data-efficient and less invasive—policies trained in this manner do not fare well in the real world (Yan et al., 2020). This is not surprising, because creating a controlled environment for

a complex, evolving system can be as large an undertaking as building the system itself (Floyd & Paxson, 2001; Bartulovic et al., 2017), making this approach prone to modeling mismatches that bias the final policy (Floyd & Paxson, 2001).

A mismatch can occur when the live system encounters an environment that was previously unseen in the controlled setting or in prior data. This is a common occurrence in real-world systems, which are time-varying, *non-stationary* environments subject to considerable changes: for example, shifting read/write patterns in databases, fluctuating bandwidth in video streaming, resizes or migrations in cloud resources, churn in competing flows in datacenter networks, and so on. To circumvent this mismatch, therefore, it is appealing to carry out reinforcement learning *in-situ*, i.e., by interacting with the live system. However, training an agent on a live system introduces several challenges.

First, an agent interacting with a new environment will inevitably incur suboptimal performance, because it has not trained on the environment before. This could endanger the system and lead to catastrophic performance loss. Second, adapting to new environments requires continual reinforcement learning, which is non-trivial (Khetarpal et al., 2020)—simply retraining the agent on new data is not sufficient. Reinforcement learning follows a two stage training procedure: during *exploration*, different actions are evaluated to learn their associated rewards, and during *exploitation*, this evaluation is used to make optimal decisions. If the environment is constantly changing, then a reinforcement learning agent must also continually explore.

---

<sup>1</sup>Computer Science and Intelligence Lab, Massachusetts Institute of Technology, Cambridge, Massachusetts, USA <sup>2</sup>Computer Science Department, Brown University, Providence, Rhode Island, USA <sup>3</sup>Microsoft Research, New York City, New York, USA. Correspondence to: Pouya Hamadani <pouyah@mit.edu>.

But the agent is only beneficial when it is exploiting its knowledge. Furthermore, training in a new environment may lead to forgetting older ones, also known as *catastrophic forgetting* (McCloskey & Cohen, 1989). Left unattended, this would necessitate retraining the agent on every change in the system, even on environments that have been observed and trained on numerous times before.

An ideal reinforcement learning agent would explore exactly as much as necessary, and exploit from that point onwards, until the environment shifts to a new dynamic. This agent would retain all of its knowledge forever, and would never need to retrain on the same environment twice.

We propose a framework to realize this goal (§5). Our framework includes an environment detector that identifies new environments, and uses this to trigger exploration when necessary. To retain knowledge about all environments, the framework trains an ensemble of expert policies, each tailored to a specific environment. To protect the system during exploration, the framework uses a safety monitor to check for a given unsafe condition, and reverts to a default policy (that is known to be safe) when this condition arises. These techniques have appeared individually in prior work (§2). However, our goal is to synthesize a complete framework for online RL and understand how well it performs in practical system optimization problems.

We evaluate our framework on two systems problems, using a combination of real-world and synthetic data: straggler mitigation in job scheduling (§6), and bitrate adaptation in video streaming (§7). We find that our framework captures and avoids notable failure modes, resulting in a robust decision learning paradigm. We believe a successful application of reinforcement learning in the wild must address the challenges discussed in this paper. To our knowledge, this is the first study of reinforcement learning in non-stationary environments in the context of systems optimization.

## 2 RELATED WORK

**Non-stationarity in Reinforcement Learning (RL):** Non-stationarity has been explored in RL in various contexts with varying assumptions, but a general solution has not been proposed (Khetarpal et al., 2020). One class of methods train meta models prior to deployment, and use few-shot learning to adapt after deployment (Nagabandi et al., 2019b; Al-Shedivat et al., 2018; Nagabandi et al., 2019a). Notably, (Nagabandi et al., 2019b) use a Chinese restaurant process and expectation maximization to model non-stationary environment dynamics, and for training with model-based RL methods. Such methods require access to the non-stationary environments before deployment, which we do not assume.

General methods for detecting environment changes have been proposed (da Silva et al., 2006; Alegre et al., 2021).

Although promising, these methods are either confined to discrete state spaces (da Silva et al., 2006), or assume Gaussian priors on transition dynamics and piece-wise stationary environments (Alegre et al., 2021). Further, it is not clear if these methods are robust to incorrect environment detections, inevitable in a realistic setting. A different approach assumes the number of models required beforehand, and decomposes a task according to its state space and time using a responsibility signal (Doya et al., 2002). For each subspace in the environment, one model learns environment dynamics, its prediction accuracy forms the responsibility signal and is used to derive a policy for that subspace. For a comprehensive review of non-stationary RL, refer to (Khetarpal et al., 2020).

**Safety in RL:** Safe RL takes on many definitions (Garcia & Fernández, 2015). Our focus is on avoiding disastrous performance outcomes in a live system while exploring (and also while exploiting). (Mao et al., 2019b) consider using a safeguard policy that is activated when safety conditions are violated, while imposing little to no bias on the agent’s training. (Rotman et al., 2020) try to detect when an agent is prone to mistakes in an online setting, and revert to a default policy afterwards. (Dalal et al., 2018) use logged data to learn when a set of constraints can be violated, and disallow the agent from taking such actions in deployment. (Achiam et al., 2017) propose an approach to keep the policy within constraints, subject to policy regularity assumptions. One of the constraints they examine partitions the state space into safe and unsafe states. (Chandak et al., 2020) seek safety in non-stationary environments by updating the policy only when improvement is ensured, under the assumption that non-stationary policy performance is smooth in time. This assumption does not hold in many realistic environments, including the ones discussed in this paper. For a full review of safety in RL, refer to (Garcia & Fernández, 2015).

One could alternatively use logged interaction data from a deployed policy, to bootstrap a safe optimal policy for deployment (Thomas, 2015; Garcia & Fernández, 2015). However, even with the assumption that logged data completely covers the entire state space (which is often unrealistic in practice), such methods are haunted by distributional shifts caused by differences between the training and testing environments (Levine et al., 2020).

**Catastrophic forgetting (CF) in RL:** Learned models are prone to catastrophically forgetting their previous knowledge when training sequentially on new information (McCloskey & Cohen, 1989; Parisi et al., 2019). Recently, interest has piqued concerning CF in RL problems. Three general approaches exist for mitigating the problem (Parisi et al., 2019): (1) regularizing model parameters so that sequential training does not cause memory loss (Kirkpatrick et al., 2017; Kaplanis et al., 2018); (2) selectively training parameters for each task and expanding when necessary (Rusu et al.,

2016b); (3) using experience replay or rehearsal mechanisms to refresh previously attained knowledge (Atkinson et al., 2021a; Rolnick et al., 2019; Isele & Cosgun, 2018); or combinations of these techniques (Schwarz et al., 2018). For a full review of these approaches, refer to (Parisi et al., 2019).

### 3 PRELIMINARIES

We first discuss how to formulate decision making problems in an RL setting, and then briefly discuss two types of RL algorithms we use throughout the paper.

#### 3.1 Markov Decision Process (MDP)

An RL problem consists of an *environment*, which is a dynamic control system modeled as an MDP (Sutton & Barto, 2018), and an *agent*, which is the entity affecting the environment through a sequence of decisions. The agent observes the environment’s *state*, and decides on an *action* that is suitable to take in that state. The environment responds to the action with a *reward* and then transitions to a new state. Formally, at time step  $t$  the environment has state  $s_t \in \mathcal{S}$ , where  $\mathcal{S}$  is the space of possible states. The agent takes action  $a_t \in \mathcal{A}$  from the possible space of actions  $\mathcal{A}$ , and receives feedback in the form of a scalar reward  $r_t(s_t, a_t) : \mathcal{S} \times \mathcal{A} \rightarrow \mathbb{R}$ . The environment’s state and the agent’s action determine the next state,  $s_{t+1}$ , according to a transition kernel,  $T(s_{t+1} | s_t, a_t)$ , which provides the distribution of the next state conditioned on the current state and action. Finally,  $d_0$  defines the distribution over initial states ( $s_0$ ). An MDP is fully defined by the tuple  $\mathcal{M} = (\mathcal{S}, \mathcal{A}, T, d_0, r)$ .<sup>1</sup> The goal of the agent is to optimize the *return*, i.e. a discounted sum of rewards  $R_0 = \sum_{t=0}^{\infty} \gamma^t r_t$ .

#### 3.2 RL algorithms

In this paper we focus on two classes of model-free RL algorithms (Sutton & Barto, 2018), which are the most commonly used approaches in RL-based systems: *on-policy* and *off-policy* algorithms. Model-free algorithms are the most common approach in RL-based systems, since they avoid the need to model the environment’s dynamics, which is difficult (and often infeasible) in real-world systems (Mao et al., 2016).

**On-policy RL:** To train an RL agent with an on-policy method, we start by deploying an initial policy to interact with the system. Each interaction creates a sample *experience* (a tuple comprising of a state, action, reward, and next state), and once enough samples are collected, the agent is trained for a single step. Importantly, the collected samples are discarded once they have been used to update the policy. This is the main limitation of on-policy methods: a policy

can only be trained on samples created by the same policy. Operationally, the implication is that such methods require a substantial amount of interaction with the live system for training, and they are inherently prone to forgetting past behaviors because they discard old experience data.

In this paper, we consider Advantage Actor Critic (A2C), a prominent on-policy algorithm (Mnih et al., 2016) based on policy gradients. We refer the reader to §A.1 in the appendix for a brief explanation of this approach.

**Off-policy RL:** Unlike on-policy methods, off-policy approaches can use samples from a policy different from the one being trained. Thus, we can use historical data to train, despite this data coming from a different policy (e.g., an earlier policy used during training). Off-policy methods maintain a record of previous interactions (also called an experience replay buffer) and use them for training. Naturally, these methods are more sample-efficient than their on-policy counterparts, but they are also known to be more prone to unstable training, suboptimal results, and hyper-parameter sensitivity (Haarnoja et al., 2018; Duan et al., 2016; Gu et al., 2016).

The most popular off-policy deep RL method is the Deep Q Network (DQN) algorithm (Mnih et al., 2013); we consider a variant of it in this paper. For more explanations regarding DQN, refer to §A.2 in the appendix.

### 4 CHALLENGES OF NON-STATIONARY RL

This section explores the key challenges that arise when using RL to train an agent in a time-varying, or non-stationary, environment. As a motivating example, we consider the problem of mitigating stragglers in an online service by “hedging” requests—i.e., replicating a request when a response doesn’t arrive within a timeout, covered in depth in §6. For the sake of this section, the important fact is that the system is subject to time-varying *workloads*, as illustrated in Figure 1. These workloads determine how the agent’s decisions affect the system: e.g., a certain timeout threshold for request hedging may be beneficial for one workload, but lead to congestion in another. The active workload in each period of time is indicated at the bottom of Figure 1. The curves in the figure show the tail of job latencies over time (note the logarithmic scale), with the objective of minimizing this latency.

**Offline training is insufficient:** Suppose we obtain a faithful simulator for the system, use it to train a policy, and then deploy the policy in the live system. We can compare such a pre-trained offline policy to a hypothetical “oracle” RL policy, which knows the workload that will appear in each interval, and uses a policy trained specifically for that workload ahead of time. Figure 1 demonstrates that the pre-trained offline agent performs significantly worse than this oracle: 188% higher tail latency in one workload and 38% in another. This is caused by the differences between the training environment

<sup>1</sup>In many problems, the agent cannot observe the full state  $s_t$  of the environment. These problems can be modeled as Partially Observable Markov Decision Process (POMDP)s, in which the agent observes a limited observation  $o_t$  instead.

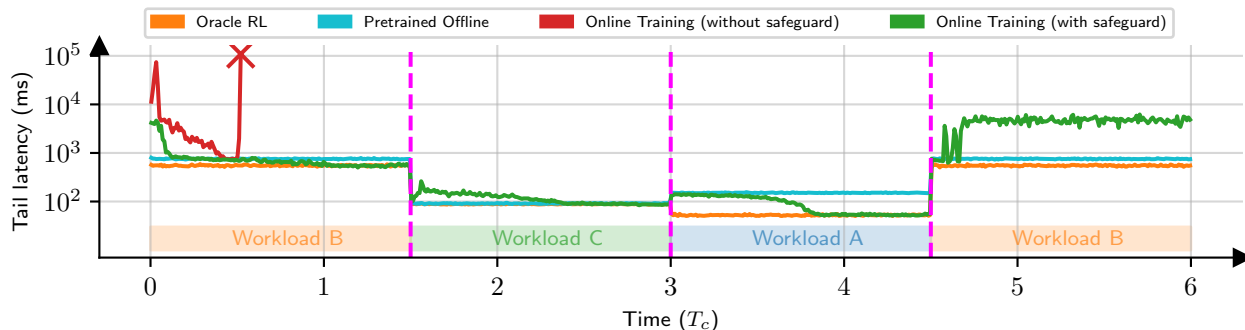


Figure 1. An example demonstrating the challenges of learning a straggler mitigation policy in an environment with time-varying workloads. Curves denote the 95<sup>th</sup> percentile job latency over 5 minutes windows.  $T_C$  denotes the convergence time when training on a stationary workload. Active workloads are marked and colored below the curves and vertical dashed lines denote workload changes.

and deployment environment (Christiano et al., 2016; Rusu et al., 2018); in this example, pre-trained offline was trained on a different workload (*OneStore*, see §B.1 for details). Although one can try to create representative training datasets, it is difficult, if not impossible, to anticipate and capture every behavior that can occur in a live system (Yan et al., 2020).

**Online RL requires safeguards:** In principle, one can avoid these issues by training an RL agent online in the live system, adapting it on the go. But this introduces other problems. As discussed earlier, RL training involves two phases: exploration and exploitation. During exploration, the agent aims to test and evaluate a wide range of actions, including both good and bad actions. It then exploits what it has learned to select favorable actions.

Online exploration in a live system can degrade performance, and possibly drive the system to disastrous states. This is shown by the “online training without safeguards” curve in Figure 1. Without a safety mechanism to keep things in check, the tail latency can shoot up and even grow without bound. Recent work has proposed using safeguards to mitigate the damage of online exploration and the instabilities that can occur during RL training (Mao et al., 2019b). A simple safeguard in Figure 1 is to disable hedging when tail latency exceeds a certain threshold (see §6 for details). Using this method, “online training with safeguards” attains stable exploration: the tail latency remains bounded throughout.

**Learning new behaviors without forgetting the past:** To learn new behaviors when the environment (workload) changes, we need to explore again. However, perpetually exploring on every change is not desirable, because even with safeguards, exploration incurs a performance cost. Ideally, we should explore sparingly, i.e., once for each new workload. In Figure 1, “online training with safeguards” tracks environment changes and initiates an exploration phase that lasts for one  $T_C$  (period of convergence, see Figure 1) the first time it encounters a new workload. Accordingly, the tail latency initially degrades when a new workload begins, and then

improves as the agent shifts from exploration to exploitation.

Figure 1 shows another challenge for online RL, however. Ideally, when workload B appears a second time, the agent should be able to immediately exploit its past knowledge. But the results show that “online training with safeguards” fails to remember what it had learnt. This is rooted in the fact that neural network-based policies forget the past when learning sequentially (McCloskey & Cohen, 1989; Parisi et al., 2019; Atkinson et al., 2021a). Specifically, when a neural network is updated based on experiences derived from one workload for a long time, it tends to overfit to the data distribution of that workload, and forgets behaviors learned from earlier data. This problem is called catastrophic forgetting (CF).

## 5 FRAMEWORK OVERVIEW

Successful deployment of RL in non-stationary systems is challenging, as evident in §4. In this section, we outline a framework, visualized in Figure 2, that serves as a blueprint for training RL agents in a live system. Our framework consists of three key modules: a safety monitor, a default policy, and an environment detector, all defined by the system designer. The *safety monitor* checks for violation of a safety condition as the agent interacts with the environment. The *default policy* is an existing scheme that, when activated in an unsafe regime, can return the system to safe operation. The *environment detector* aims to detect which environment is active at any given time. It typically takes in a small set of features (selected by the system designer) and uses them to detect changes in the environment. For instance, to detect changes in the workload, we might use features such as job arrival rates and job types. We now discuss how our framework addresses the three challenges described in §4.

**Safety:** Safety is handled in a straightforward way in our framework. As shown in Figure 2, the safety monitor controls whether the agent or the default policy decides the next action. When in an unsafe state, the default policy is activated, which drives the system to a safe region before control is given

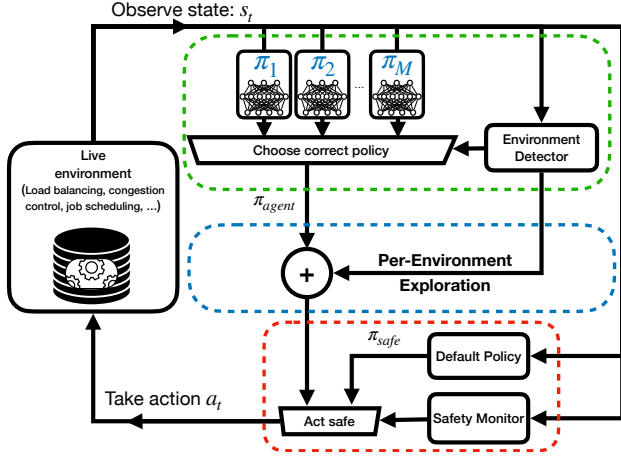


Figure 2. Framework overview for non-stationary RL. Green components mitigate catastrophic forgetting, Blue components concern per-environment exploration, and Red components deal with safety.

back to the RL agent to resume training. This limits the performance impact of exploration or other misbehaviors by the RL agent (e.g., transient policy problems during training).

**Per-Environment Exploration:** As each environment has its own dynamics, knowledge attained by exploring in one environment may not generalize to others. Thus, for each observed environment, we initiate a one-time exploration. The choice to explore can be driven by the environment detection signal, as shown in Figure 2. We believe that in many systems, the cost of per-environment exploration (with safeguards) is justified by the lifelong performance improvement. As the agent collects more experience, we expect it to encounter new environments less frequently over time, and thus spend most of its time exploiting past knowledge. An alternative strawman approach that we considered is to continually use a small level of exploration all the time. However, prior work (Ahmed et al., 2019) and our initial experiments showed that this leads to poor policies and is difficult to tune appropriately.

**Catastrophic forgetting:** Forgetting past knowledge stems from training a single policy with recent data that is devoid of old experiences. We adopt a simple solution that avoids this problem altogether by training different policies for each environment, also referred to as multiple “experts” (Rusu et al., 2016a). We select the appropriate expert to use and train in each environment using the environment detector. Our results suggest that this approach can be quite effective, even when the environment detector isn’t perfect and makes mistakes. We also investigate an alternate approach that uses off-policy RL to train a single model based on an experience replay buffer. While this approach can also mitigate CF (since the buffer allows the agent to replay past experiences), we found it to be less robust than the multi-expert approach.

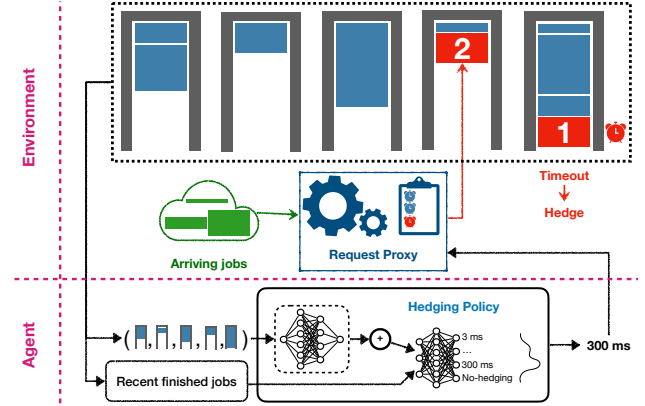


Figure 3. Illustration of a request proxy with hedging.

## 6 CASE STUDY: STRAGGLER MITIGATION

We consider a simulated request proxy with hedging (Figure 3). In this environment, a proxy receives and forwards requests to one of  $n$  servers. The servers process requests in their queues one by one. To load balance, the proxy sends the request to the server with the shortest queue. To respond to a request, the server launches a job that requires a nominal processing time, which we will refer to as its size. The size of a job is not known prior to it being processed. Henceforth we will use the terms “request” and “job” interchangeably.

In a real system, some jobs may incur a slow down and take longer than the nominal time, e.g., due to unmet dependencies, IO failure, periodic events such as garbage collection (Dean & Barroso, 2013), noisy neighbours (Pu et al., 2010), etc. These slowdowns also affect other jobs further in the queue. The effect is especially pronounced at the tail of job latency, which is the time between the job’s arrival and its completion. To simulate such behaviors in our environment, we inflate the processing time of a job relative to the nominal value by a factor of  $k$  with a small probability  $p$ . We use  $k = 10$  and  $p = 0.1$  in our experiments.

To mitigate the effect of slowdowns, if a job has not completed by a timeout, the proxy “hedges” it by sending a duplicate request to another server. This duplication only happens once per job. The job completes when either request (the original or its duplicate) finishes. If the hedged request finishes faster than the original one, the job’s latency is reduced. Our goal is to minimize the 95<sup>th</sup> percentile latency, and our control decision is the hedging timeout. The hedging policy gets to pick among a set of six timeout values, ranging from 3<sup>ms</sup> to 300<sup>ms</sup>, or alternatively to do no hedging.

There is an inherent trade off in selecting a hedging timeout. A low timeout leads to more jobs being hedged, possibly reducing their latency, but it also creates more load on the system, resulting in bigger queues. An RL agent can learn the optimal threshold, which depends on the workload (e.g., the job arrival rate and job sizes) and the amount of

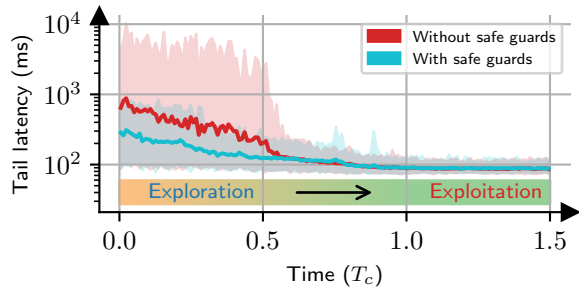


Figure 4. Tail latency over time in workload C, when using a safe guard to reduce performance loss in exploration, and when not. Shaded regions denote tail latency min-to-max in 3 random seeds.

congestion (e.g., queue sizes) in the system. Since these change over time, this environment is non-stationary.

As nothing is known about jobs prior to processing, it doesn’t help to make individual decisions on a per-job basis. Instead, the agent chooses one hedging timeout for all jobs that arrive within a time window (500 ms in our experiments). It makes these decisions using the following observations: (a) instantaneous server queue sizes, (b) average server queue sizes over the last time window, (c) average and max of job processing times and rate of incoming jobs within  $m = 4$  time windows, (d) the average load in the last time window, and (e) whether a safeguard is active (more details below). The reward is the negated 95<sup>th</sup> percentile latency of jobs in that window.

With  $n$  servers, the observation includes  $2n$  dimensions regarding instantaneous and average queue statistics. These statistics are in essence a set, and the order they appear in the observation does not matter, e.g., if queue 4 comes before queue 8 or vice versa. We therefore use the DeepSets (Zaheer et al., 2018) architecture to create permutation-invariant neural network models that exploit this structure. At a high level, this architecture works by learning an embedding function applied to each queue’s statistics, and summing the resulting embeddings to represent the set of queue statistics. §B.3 has a full description of our training setup and environment.

**Safeguard:** We use a safeguard policy (Mao et al., 2019b) to improve transient performance and stabilize training. The safeguard overrides the agent when at least one queue builds up past a threshold (50) and disables hedging while in control. It relinquishes control back to the RL agent once all queue sizes are below a safe threshold (3).

**Workloads:** We use traces from a production web framework cluster at AnonCo, collected from a single day in February 2018. The framework services high-level web requests to different websites and storefront properties and routes them to various backend services (e.g., product catalogs, billing, etc.). The traces are noisy, heavily temporally-correlated, and change considerably over time, as Figures 15 and 17 in the appendix demonstrate. See §B.1 for more details about this workload.

For experiments in non-stationary settings, we consider a scenario where several workloads (*Workload A, B and C* from Figure 17) change according to a schedule (scenario I in Figure 7). Specifically, workloads change in a periodic and cyclic manner, each active for a period of  $T_{sw}$  at a time. In all experiments, we run this scenario with different permutations of workloads (e.g., *ABC, BCA, CBA*, etc.), as the order of workloads can affect RL training schemes. The period between switches,  $T_{sw}$  is relative to convergence time  $T_c$  of an RL agent trained for only one workload. While not particularly realistic, periodic and abrupt workload changes provide a simple setting to understand the strengths and weakness of different online RL strategies.

**Evaluation metric:** For evaluation, we calculate the 95<sup>th</sup> percentile latency in 5 minute windows. We use this tail latency metric in all experiments, by either plotting it as a timeseries, or by visualizing its distribution with boxplots.

## 6.1 Experiments

**Safeguards bound performance degradation during exploration:** As discussed before, training online in a live system requires online exploration, which leads to transient loss in performance. While our main priority is to achieve strong eventual performance, bounding transient degradation while exploring is a secondary but important goal. We achieve this using safeguard policies, as explained in §5. Figure 4 demonstrates the effect. Without safeguards, latencies can be an order of magnitude higher than the worst case performance with safeguards.

We observed that occasionally training sessions without safeguards failed to learn at all and queues grew beyond tens of thousands of jobs. Figure 1 showed an example of such a failure mode. This occurs because when queues exceed a certain bound, all jobs will take longer than the maximum hedging timeout (300 ms) and get duplicated. In such a situation, the only way to drain the queues is to disable hedging entirely. But while the agent tries to learn this behavior, the queues continue to grow and the system repeatedly reaches states that the agent has never seen before. Hence, the agent is not able to spend enough time exploring the same region of the state space to learn a stabilizing policy and a vicious cycle forms.

**Exploration is critical with new workloads:** In §5 we stated that every time the workload changes, we need to explore again. This requires designing an environment detector and switching to the exploration phase whenever a change is observed. In this environment, detecting changes is relatively simple. We use two features: the job arrival rate and the job sizes to characterize the workload (as shown in Figure 17). By tracking these features, we can cluster our workloads and train a classifier for them. Of course, the classifier may not be perfect, e.g., the clusters may overlap and not be completely separable. But our experiments show that this simple

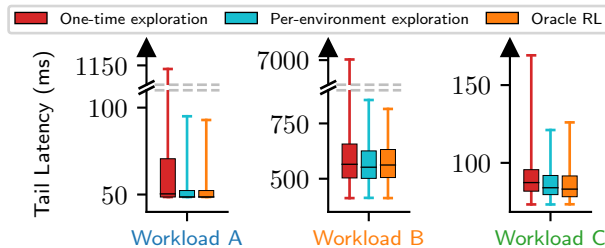


Figure 5. Tail latency distribution after convergence; Each box represents one of the workloads. Whiskers show 99 and 1 percentiles. Upper, middle and lower edge of boxes show 75, 50, and 25 percentiles. Each workload is given enough time to converge ( $T_{sw} = 2.25T_c$ ).

approach is adequate. It is possible to design more complex features and clustering schemes, but the exact approach to designing an environment detector is not our focus in this work.

Figure 5 demonstrates the effect of exploring once for each workload. Each boxplot shows tail latency distributions for one of three workloads (across different experiments in which we permute the workload order). The boxes show the 25<sup>th</sup>, median and 75<sup>th</sup> percentiles of the distributions and whiskers denote 1<sup>st</sup> and 99<sup>th</sup>. While one-time exploration (for  $T_c$  time) fails to handle new workloads, per-environment exploration converges to a good policy for each workload. Figure 16 in the appendix shows an example of how the tail latency varies over time with these approaches.

**Catastrophic Forgetting:** The largest obstacle to online learning is CF. As observed in Figure 1, sequential training will cause a single model to forget its previous training. We evaluate two techniques to mitigate CF: (1) Providing features as part of the agent’s observation that enable it to distinguish between different workloads. By adding these features, the agent can potentially use a single model while learning different behaviors for different workloads. For this scheme, we use the same features used by our workload classifier. (2) Employing multiple experts, each trained and used for a unique workload, as explained in §5. Ideally the expert for workload A will never be used for and trained in workload B, thus never forgetting the policy it learned for workload A. In practice, the environment detector will however make mistakes, but we found that even a 10% error rate will not degrade performance.

In Figure 6, we evaluate multiple experts vs. a single one, and the impact of providing workload features in the observation for both approaches. We consider two different switching periods between workloads:  $T_{sw} = T_c$  (slow switching) and  $T_{sw} = 0.001 T_c$  (fast switching). As a baseline, we also include results for Oracle RL that uses trained policies specific to each workload.

Figure 6a concerns situations where workload changes occur at long periods. In these cases multiple experts significantly outperform a single expert, even when workload information

is included in the observations. Workload features don’t help in this case since they remain roughly constant throughout the convergence interval of the RL algorithm. On the other hand in Figure 6b where workloads change rapidly, the single model with workload features matches multiple experts. When workloads change at a fast pace, the agent gets to observe samples from all environments (with different workload features) as the RL algorithm converges. Note that in this case the multiple-expert scheme’s performance is worse without workload information; this is due to environment classification errors caused by stale information. However, multiple experts with workload information manages to perform well despite these errors since each expert learns to handle observations from non-matching workloads as well. Overall, multiple experts with workload information is robust in all cases.

Multiple experts are not the only solution for CF and a rich variety of methods have been proposed (Atkinson et al., 2021b; Rusu et al., 2016b; Kirkpatrick et al., 2017). Such methods might enable sharing knowledge learned from one workload for training another. However, multiple experts has the advantage of being robust and simple to design and interpret.

**Can we avoid catastrophic forgetting with a single model with off-policy methods?** As explained in §3, off-policy methods such as DQN can train on historical samples using an experience replay buffer. Therefore perhaps an off-policy approach can avoid CF even with a single model. Using a single model simplifies the agent and could accelerate learning by enabling shared learning across workloads.<sup>2</sup>

While appealing, off-policy schemes have their own challenges. In particular, their performance is sensitive to the samples saved in the experience buffer, which must be selected carefully to match the mixture of workloads experienced by the agent over time. Further, as we discuss in §B.2.3, using a single model (the Q-network in DQN) across different workloads requires reward scaling to ensure some workloads with large rewards do not drown out others.

In the following experiments, we examine DQN with several buffering strategies and compare them to oracle baselines and the on-policy multiple-expert approach: a (1) **Large Buffer** that is akin to saving every sample, a (2) **Small Buffer**, which inherently prioritizes recent samples, (3) **Long-term short-term** that saves experiences in two buffers, one large and one small (Isele & Cosgun, 2018), and samples from them equally during training to combine data from the entire history with recent samples, and (4) **Multiple buffers** that keeps a separate buffer for each workload and samples equally from them during training.

Our evaluations use three workload schedules shown in Figure 7. In the on-policy experiments we focused on scenario I

<sup>2</sup>Note that we still need a workload detection scheme for per-environment exploration.

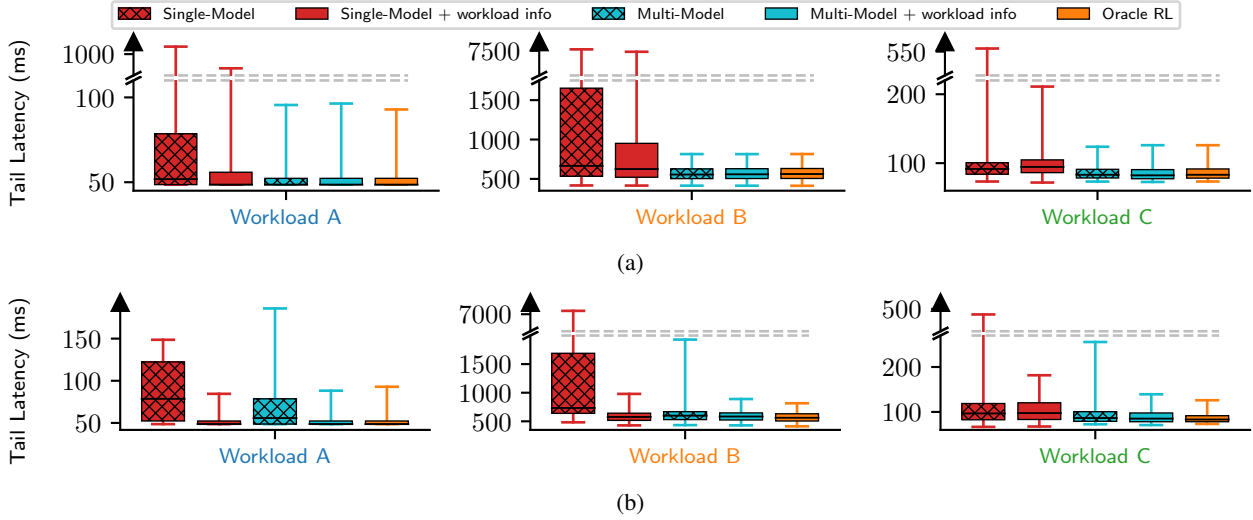


Figure 6. Tail latency distribution after convergence, when either a single model is used or multiple, and when workload statistics are observed or not. **(Top)**  $T_{sw} = T_c$  (Slow workload switching), **(Bottom)**  $T_{sw} = 0.001 T_c$  (Fast workload switching).

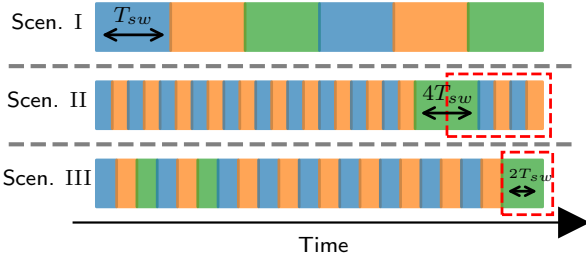


Figure 7. We evaluate three non-stationary scenarios. Scenario I: the system cycles through three different workloads, each active for  $T_{sw}$  at a time. Scenario II: two workloads occur periodically for a long time, then a new workload shows up. Scenario III: the system cycles through three workloads, one of which becomes inactive for a long time, then reoccurs.

where workloads change in a cyclic manner, but here we also consider cases where some workloads might be encountered rarely. Notably, we will find that unlike the on-policy method, the off-policy approach can be sensitive to the schedule.

Figure 8 demonstrates the results for scenario I. Unsurprisingly, a small buffer does not fare well; it loses experience samples of previous workloads and the agent forgets them, leading to CF. Also, in workload C, the DQN-based oracle fares slightly better than all other DQN methods that train simultaneously on multiple workloads. A similar observation arises in Figure 6, when using a single model with workload info at a fast workload switching setting. We believe this slight loss is due to shared learning, which can sometimes diminish performance instead of improving it when using a single neural network model for diverse tasks (Taylor & Stone, 2011).

Figure 9 shows the same set of schemes in scenario II, where a rare workload does not come up until well into training.

We use workload C as this rare workload and A and B as the common ones. The evaluations in this plot show performance after workload C converges (a region shown by the red box in scenario II in Figure 7). In chronological order, the results for workload C show the large buffer struggling; a large buffer will amass a high volume of samples after a long time and a new workload will have a minuscule share of buffer and training samples. The results for workloads A and B on the other hand exhibit the forgetfulness of a small buffer, similar to the previous experiment. Contrary to both methods, long-term short-term performs well.

Finally, Figure 10 shows results for scenario III, which demonstrates how well an approach can remember a rarely occurring workload (shown by the red box in Figure 7). Here long-term short-term does not cope well; the small buffer forgets workload C and the large one favors more common ones. Multiple buffers performed well here, but it is worse than long-term short-term in scenario II (Figure 9). Overall, these results show that none of these schemes can be a universal strategy that performs well in all circumstances. By contrast, the on-policy multiple-expert approach is more robust.

## 7 CASE STUDY: ADAPTIVE BIT RATE

We now apply the framework from §5 to the Adaptive Bit Rate (ABR) environment.

In this environment, a server streams video to a client. The video is divided into  $T$  second chunks and each chunk is encoded at several bitrates of varying quality and file size. For each chunk, an ABR algorithm decides which bitrate to send. At the client-side, a playback buffer aggregates received chunks and displays the video to the client, draining the buffer at a constant rate. Formally, at step  $t$  and when the



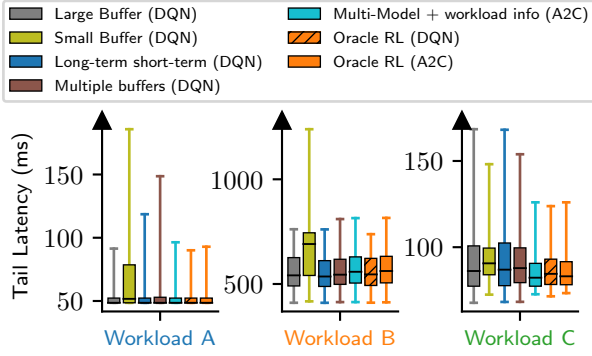


Figure 8. Tail latency distribution after convergence in Scenario I, when  $T_{sw} = T_c$  (similar to Figure 6). DQN with a small buffer forgets past workloads.

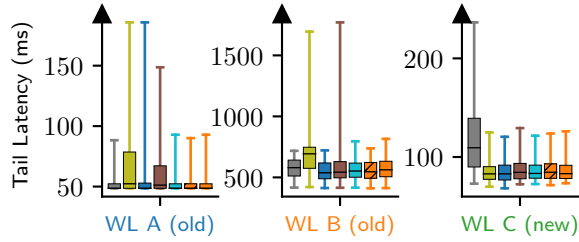


Figure 9. Tail latency distribution after convergence in Scenario II, when  $T_{sw} = 0.5T_c$ . Left and middle plot concern remembering common workloads after training on a new one. Right plot shows performance on a new workload, after convergence time ( $T_c$ ). Large and small buffers fail while long-term short-term uses the best of both to fare best.

clients buffer is  $b_t$ , the server streams the next video chunk with size  $S_t$  and bandwidth  $c_t$ . If the chunk arrives after the buffer depletes, the video pauses and the client observes a *rebuffer event*. Generally, the next buffer will be:

$$b_{t+1} = \max(0, b_t - \frac{S_t}{c_t}) + T$$

The client only requests chunks when the buffer falls below threshold  $M_b$ . There are three goals in this environment; **avoid rebuffer events**, **stream in high quality**, and **maintain a stable quality**. These goals are conflicting in nature, and systems in practice optimize a linear combination of them, coined Quality of Experience (QoE) (Yin et al., 2015)<sup>3</sup>. Assuming the bitrate of step  $t$  was  $q_t$ , the QoE is:

$$QoE_t = q_t - |q_t - q_{t-1}| - \mu \cdot \max(0, \frac{S_t}{c_t} - b_t)$$

To learn a policy for this problem, we have to define the observations, reward and actions. Each step in the

<sup>3</sup>There are numerous methods for defining QoE metrics (Mao et al., 2017; Spiteri et al., 2020; Yin et al., 2015). The choice of QoE is orthogonal to our discussion.

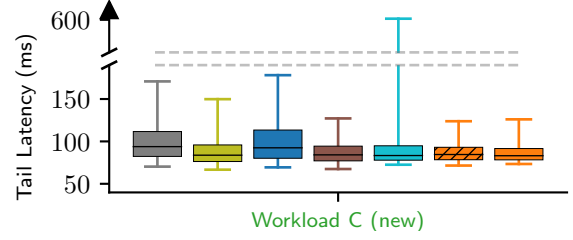


Figure 10. Tail latency distribution after convergence in Scenario III, when  $T_{sw} = 0.5T_c$ . This plot concerns how well an agent remembers a rarely occurring workload. Long-term short-term is outperformed by multiple buffers.

Group	Average BW	Individual variance	Diversity
UG 1	Low	High	Medium
UG 2	High	Low	High
UG 3	Medium	Medium	Low
UG 4	Medium-Low	Medium	Low
UG 5	Medium	High	Very High

Table 1. High level description of User Groups. Refer to §C.1 in the appendix for further details.

environment is a video chunk and the action is what bitrate is sent. The reward is the QoE of that chunk. The observation  $o_t$  is comprised of (a) download times and bandwidths in the last  $K = 9$  chunks, (b) buffer occupancy before sending chunk  $t$ , (c) how many chunks are left in the video, (d) the previous chunk’s bitrate (previous action) and (e) available bitrates for chunk  $t$ . For more details on the ABR environment and training setup, see §C.3.

The network path distribution of active streaming sessions is the non-stationary element in this problem. A server responds to and shares a single learned policy for all clients, but the users of the service will change over time (e.g., children in the morning and adults at night at a daily scale, and events such as streaming sports or election news at a weekly/yearly scale). With them, the network path distribution of active sessions changes. The networks themselves can also change: e.g., cellular use in mornings and broadband at night. Further, changes such as new network infrastructure and protocols affect network sessions. To model this, we switch between one of five bandwidth distributions from a generative model, similar to scenario I (see Figure 7). Table 1 provides a high level description of how these groups differ. For details about these distributions and sample bandwidth traces, see §C.1.

## 7.1 Safe guard policy

Transient performance is important in the video streaming setting. If the RL agent’s exploration phase causes significant rebuffering, user satisfaction will drop. Figure 19 shows how much rebuffering is caused by A2C while training. In initial exploration stages, A2C rebuffers as long as the video

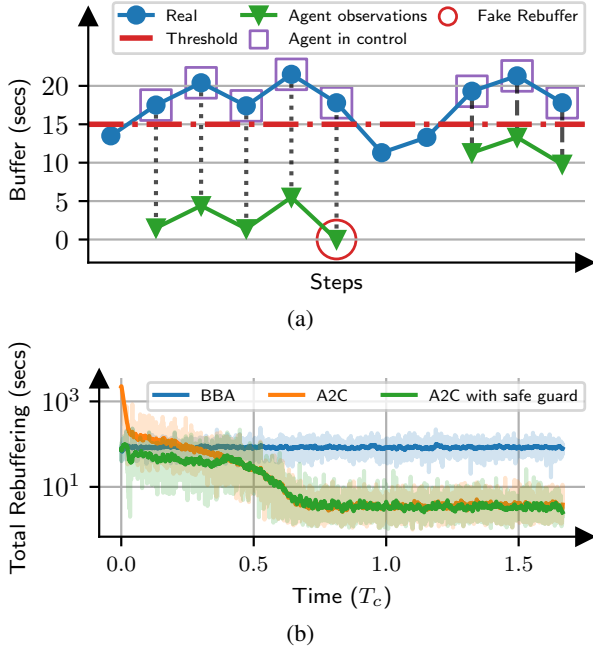


Figure 11. (a) An example of how the safe guard operates. (b) Total rebuffering across time, for three variants, under user group 1. Note that the y-axis is logarithmic, due to wide range.

length, while by the end rebuffering is in the range of a few seconds. Thus, we design a safe-guard policy for ABR training, similar to the one introduced in §6.

A natural idea is to gradually give control to the agent, i.e., start it off with control over a limited number of chunks and, after convergence, give full control. The primary goal is to avoid rebuffering, so we can give control to the agent when rebuffering is less likely (e.g., when buffer occupancy is high). Hence, we give control to the agent whenever the buffer occupancy is above a threshold (the red line in Figure 11a). For buffer levels below the threshold, we use a reliable but sub-optimal algorithm like Buffer Based Approach (BBA) (Huang et al., 2014). We then slowly anneal the threshold to promote the agent to full control.

This creates an issue: the agent’s exploration phase is biased towards high buffer states, and the agent fails to learn how to behave in risky low buffer situations. To mitigate this, we fool the agent into thinking the buffer is at a lower value. Note that since the buffer dynamics in ABR are simple, this is possible in a real system. Whenever the agent gains control from the safe guard, a buffer value is chosen uniformly at random from the safe guard, a buffer value is chosen uniformly at random from the actual buffer and 0. The agent’s following observations will be based on this initial buffer value. Figure 11a provides a visual example. This ruse continues until the real buffer falls below the threshold and the safe guard takes over.

Figure 11b compares A2C with Fake-Replay, A2C and BBA, while the RL agents are training over a challenging bandwidth distribution. As observed, A2C with no

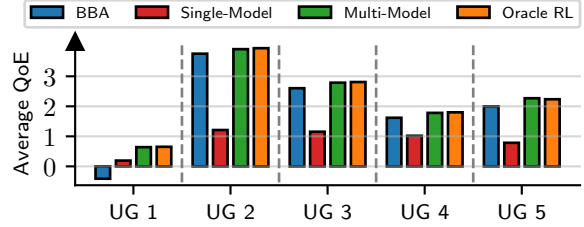


Figure 12. Average QoE after convergence in Scenario I when  $T_{sw} = T_c$ , per different user groups.  $UG X$  refers to *User Group X*. Higher is better.

safeguards begins training with significant rebuffering, but over time learns to rebuffer even less than BBA. A2C with Fake-Replay does not rebuffer overwhelmingly like A2C, and its final performance is unaffected by the safe-guard.

## 7.2 Multiple experts against non-stationary users

We designed a reliable safe guard in §7.1. To detect user distributions (environment contexts), we use the same trained classifier approach as before. This classifier looks at the average bandwidth and its variability at two time scales. We use this classifier to dynamically control the exploration. A2C with multiple experts proved reasonably robust in the previous case study and therefore we use this approach here.

Figure 12 compares BBA, a single expert and an oracle baseline against the multiple expert approach. We consider BBA as a non-learning based alternative. As observed, multiple experts’ results are similar to the oracle, which means the multiple experts approach has completely side-tracked non-stationarity. Also, the multiple experts approach achieves favorable results compared to BBA, while the single expert baseline does not. This implies that without dealing with non-stationarity, utilizing learned policies via RL will not be practical. By considering this important aspect, evident in many real-world problem, one can truly utilize the benefits of RL. For a breakdown and interpretation of these QoE results, see §C.2.

## 8 CONCLUSION

We investigated the challenges of online RL in non-stationary systems environments, and proposed a framework to address these challenges. Our work shows that an RL agent must be augmented with several components in order to learn robustly while minimally impacting system performance. In particular, we propose an environment detector to control exploration and select an appropriate model for each environment; and we also propose a safety monitor and default policy that protect the system when it enters an unsafe condition. Our evaluation on two systems problems, straggler mitigation and bitrate adaptation, shows that applying our framework leads to policies that perform well

in each environment and remember what they have learned.

## REFERENCES

- Achiam, J., Held, D., Tamar, A., and Abbeel, P. Constrained policy optimization, 2017.
- Ahmed, Z., Roux, N. L., Norouzi, M., and Schuurmans, D. Understanding the impact of entropy on policy optimization, 2019.
- Akhtar, Z., Nam, Y. S., Govindan, R., Rao, S., Chen, J., Katz-Bassett, E., Ribeiro, B., Zhan, J., and Zhang, H. Oboe: Auto-tuning video abr algorithms to network conditions. In *Proceedings of the 2018 Conference of the ACM Special Interest Group on Data Communication, SIGCOMM '18*, pp. 44–58, New York, NY, USA, 2018. Association for Computing Machinery. ISBN 9781450355674. doi: 10.1145/3230543.3230558. URL <https://doi.org/10.1145/3230543.3230558>.
- Al-Shedivat, M., Bansal, T., Burda, Y., Sutskever, I., Mordatch, I., and Abbeel, P. Continuous adaptation via meta-learning in nonstationary and competitive environments, 2018.
- Alegre, L. N., Bazzan, A. L., and da Silva, B. C. Minimum-delay adaptation in non-stationary reinforcement learning via online high-confidence change-point detection. In *Proceedings of the 20th International Conference on Autonomous Agents and MultiAgent Systems*, pp. 97–105, 2021.
- Atkinson, C., McCane, B., Szymanski, L., and Robins, A. Pseudo-rehearsal: Achieving deep reinforcement learning without catastrophic forgetting. *Neurocomputing*, 428:291–307, Mar 2021a. ISSN 0925-2312. doi: 10.1016/j.neucom.2020.11.050. URL <http://dx.doi.org/10.1016/j.neucom.2020.11.050>.
- Atkinson, C., McCane, B., Szymanski, L., and Robins, A. Pseudo-rehearsal: Achieving deep reinforcement learning without catastrophic forgetting. *Neurocomputing*, 428: 291–307, 2021b.
- Bartulovic, M., Jiang, J., Balakrishnan, S., Sekar, V., and Sinopoli, B. Biases in data-driven networking, and what to do about them. In *Proceedings of the 16th ACM Workshop on Hot Topics in Networks*, pp. 192–198. ACM, 2017.
- Chandak, Y., Jordan, S. M., Theocharous, G., White, M., and Thomas, P. S. Towards safe policy improvement for non-stationary mdps, 2020.
- Christiano, P., Shah, Z., Mordatch, I., Schneider, J., Blackwell, T., Tobin, J., Abbeel, P., and Zaremba, W. Transfer from simulation to real world through learning deep inverse dynamics model, 2016.
- da Silva, B. C., Basso, E. W., Bazzan, A. L. C., and Engel, P. M. Dealing with non-stationary environments using context detection. In *Proceedings of the 23rd International Conference on Machine Learning, ICML '06*, pp. 217–224, New York, NY, USA, 2006. Association for Computing Machinery. ISBN 1595933832. doi: 10.1145/1143844.1143872. URL <https://doi.org/10.1145/1143844.1143872>.
- Dalal, G., Dvijotham, K., Vecerik, M., Hester, T., Paduraru, C., and Tassa, Y. Safe exploration in continuous action spaces. *arXiv preprint arXiv:1801.08757*, 2018.
- DASH Industry Form. Reference client 2.4.0, 2016. URL <http://mediapm.edgesuite.net/dash/public/nightly/samples/dash-if-reference-player/index.html>.
- Dean, J. and Barroso, L. A. The tail at scale. *Communications of the ACM*, 56:74–80, 2013. URL <http://cacm.acm.org/magazines/2013/2/160173-the-tail-at-scale/fulltext>.
- Doya, K., Samejima, K., Katagiri, K.-i., and Kawato, M. Multiple model-based reinforcement learning. *Neural computation*, 14(6):1347–1369, 2002.
- Duan, Y., Chen, X., Houthoofd, R., Schulman, J., and Abbeel, P. Benchmarking deep reinforcement learning for continuous control. In *International conference on machine learning*, pp. 1329–1338. PMLR, 2016.
- Floyd, S. and Paxson, V. Difficulties in simulating the internet. *IEEE/ACM Transactions on Networking (ToN)*, 9(4):392–403, 2001.
- Gao, Y., Chen, L., and Li, B. Spotlight: Optimizing device placement for training deep neural networks. In Dy, J. and Krause, A. (eds.), *Proceedings of the 35th International Conference on Machine Learning*, volume 80 of *Proceedings of Machine Learning Research*, pp. 1676–1684. PMLR, 10–15 Jul 2018. URL <https://proceedings.mlr.press/v80/gao18a.html>.
- Garcia, J. and Fernández, F. A comprehensive survey on safe reinforcement learning. *Journal of Machine Learning Research*, 16(1):1437–1480, 2015.
- Gu, S., Lillicrap, T., Ghahramani, Z., Turner, R. E., and Levine, S. Q-prop: Sample-efficient policy gradient with an off-policy critic. *arXiv preprint arXiv:1611.02247*, 2016.
- Haarnoja, T., Zhou, A., Abbeel, P., and Levine, S. Soft actor-critic: Off-policy maximum entropy deep reinforcement learning with a stochastic actor. In *International conference on machine learning*, pp. 1861–1870. PMLR, 2018.

- Hasselt, H. v., Guez, A., and Silver, D. Deep reinforcement learning with double q-learning. In *Proceedings of the Thirtieth AAAI Conference on Artificial Intelligence*, AAAI'16, pp. 2094–2100. AAAI Press, 2016.
- Hessel, M., Soyer, H., Espeholt, L., Czarnecki, W., Schmitt, S., and van Hasselt, H. Multi-task deep reinforcement learning with popart, 2018.
- Huang, T.-Y., Johari, R., McKeown, N., Trunnell, M., and Watson, M. A buffer-based approach to rate adaptation: Evidence from a large video streaming service. In *Proceedings of the 2014 ACM Conference on SIGCOMM*, SIGCOMM '14, pp. 187–198, New York, NY, USA, 2014. Association for Computing Machinery. ISBN 9781450328364. doi: 10.1145/2619239.2626296. URL <https://doi.org/10.1145/2619239.2626296>.
- Isele, D. and Cosgun, A. Selective experience replay for lifelong learning, 2018.
- Jay, N., Rotman, N. H., Godfrey, P. B., Schapira, M., and Tamar, A. Internet congestion control via deep reinforcement learning, 2019.
- Kaplanis, C., Shanahan, M., and Clopath, C. Continual reinforcement learning with complex synapses, 2018.
- Khetarpal, K., Riemer, M., Rish, I., and Precup, D. Towards continual reinforcement learning: A review and perspectives. *arXiv preprint arXiv:2012.13490*, 2020.
- Kingma, D. P. and Ba, J. Adam: A method for stochastic optimization, 2017.
- Kirkpatrick, J., Pascanu, R., Rabinowitz, N., Veness, J., Desjardins, G., Rusu, A. A., Milan, K., Quan, J., Ramalho, T., Grabska-Barwinska, A., et al. Overcoming catastrophic forgetting in neural networks. *Proceedings of the national academy of sciences*, 114(13):3521–3526, 2017.
- Krishnan, S., Yang, Z., Goldberg, K., Hellerstein, J., and Stoica, I. Learning to optimize join queries with deep reinforcement learning, 2019.
- Levine, S., Kumar, A., Tucker, G., and Fu, J. Offline reinforcement learning: Tutorial, review, and perspectives on open problems, 2020.
- Lillicrap, T. P., Hunt, J. J., Pritzel, A., Heess, N., Erez, T., Tassa, Y., Silver, D., and Wierstra, D. Continuous control with deep reinforcement learning, 2019.
- Mao, H., Alizadeh, M., Menache, I., and Kandula, S. Resource management with deep reinforcement learning. In *Proceedings of the 15th ACM workshop on hot topics in networks*, pp. 50–56, 2016.
- Mao, H., Netravali, R., and Alizadeh, M. Neural adaptive video streaming with pensieve. In *Proceedings of the Conference of the ACM Special Interest Group on Data Communication*, pp. 197–210, 2017.
- Mao, H., Negi, P., Narayan, A., Wang, H., Yang, J., Wang, H., Marcus, R., Addanki, R., Khani, M., He, S., et al. Park: an open platform for learning-augmented computer systems. In *Proceedings of the 33rd International Conference on Neural Information Processing Systems*, pp. 2494–2506, 2019a.
- Mao, H., Schwarzkopf, M., He, H., and Alizadeh, M. Towards safe online reinforcement learning in computer systems. 2019b.
- Mao, H., Schwarzkopf, M., Venkatakrishnan, S. B., Meng, Z., and Alizadeh, M. Learning scheduling algorithms for data processing clusters. In *Proceedings of the ACM Special Interest Group on Data Communication*, SIGCOMM '19, pp. 270–288, New York, NY, USA, 2019c. Association for Computing Machinery. ISBN 9781450359566. doi: 10.1145/3341302.3342080. URL <https://doi.org/10.1145/3341302.3342080>.
- Marcus, R., Negi, P., Mao, H., Zhang, C., Alizadeh, M., Kraska, T., Papaemmanouil, O., and Tatbul, N. Neo: A learned query optimizer. *arXiv preprint arXiv:1904.03711*, 2019.
- McCloskey, M. and Cohen, N. J. Catastrophic interference in connectionist networks: The sequential learning problem. *Psychology of Learning and Motivation*, 24:109–165, 1989. ISSN 0079-7421. doi: [https://doi.org/10.1016/S0079-7421\(08\)60536-8](https://doi.org/10.1016/S0079-7421(08)60536-8). URL <https://www.sciencedirect.com/science/article/pii/S0079742108605368>.
- Mnih, V., Kavukcuoglu, K., Silver, D., Graves, A., Antonoglou, I., Wierstra, D., and Riedmiller, M. Playing atari with deep reinforcement learning. *arXiv preprint arXiv:1312.5602*, 2013.
- Mnih, V., Badia, A. P., Mirza, M., Graves, A., Lillicrap, T., Harley, T., Silver, D., and Kavukcuoglu, K. Asynchronous methods for deep reinforcement learning. In *International conference on machine learning*, pp. 1928–1937. PMLR, 2016.
- Nagabandi, A., Clavera, I., Liu, S., Fearing, R. S., Abbeel, P., Levine, S., and Finn, C. Learning to adapt in dynamic, real-world environments through meta-reinforcement learning, 2019a.
- Nagabandi, A., Finn, C., and Levine, S. Deep online learning via meta-learning: Continual adaptation for model-based rl, 2019b.

- Parisi, G. I., Kemker, R., Part, J. L., Kanan, C., and Wermter, S. Continual lifelong learning with neural networks: A review. *Neural Networks*, 113:54–71, 2019. ISSN 0893-6080. doi: <https://doi.org/10.1016/j.neunet.2019.01.012>. URL <https://www.sciencedirect.com/science/article/pii/S0893608019300231>.
- Paszke, A., Gross, S., Massa, F., Lerer, A., Bradbury, J., Chanan, G., Killeen, T., Lin, Z., Gimelshein, N., Antiga, L., Desmaison, A., Kopf, A., Yang, E., DeVito, Z., Raison, M., Tejani, A., Chilamkurthy, S., Steiner, B., Fang, L., Bai, J., and Chintala, S. Pytorch: An imperative style, high-performance deep learning library. In Wallach, H., Larochelle, H., Beygelzimer, A., d'Alché-Buc, F., Fox, E., and Garnett, R. (eds.), *Advances in Neural Information Processing Systems 32*, pp. 8024–8035. Curran Associates, Inc., 2019. URL <http://papers.neurips.cc/paper/9015-pytorch-an-imperative-style-high-performance-deep-learning-library.pdf>.
- Pu, X., Liu, L., Mei, Y., Sivathanu, S., Koh, Y., and Pu, C. Understanding performance interference of i/o workload in virtualized cloud environments. *2010 IEEE 3rd International Conference on Cloud Computing*, pp. 51–58, 2010.
- Rolnick, D., Ahuja, A., Schwarz, J., Lillicrap, T. P., and Wayne, G. Experience replay for continual learning, 2019.
- Rotman, N. H., Schapira, M., and Tamar, A. Online safety assurance for learning-augmented systems. In *Proceedings of the 19th ACM Workshop on Hot Topics in Networks*, pp. 88–95, 2020.
- Rusu, A. A., Colmenarejo, S. G., Gulcehre, C., Desjardins, G., Kirkpatrick, J., Pascanu, R., Mnih, V., Kavukcuoglu, K., and Hadsell, R. Policy distillation, 2016a.
- Rusu, A. A., Rabinowitz, N. C., Desjardins, G., Soyer, H., Kirkpatrick, J., Kavukcuoglu, K., Pascanu, R., and Hadsell, R. Progressive neural networks. *arXiv preprint arXiv:1606.04671*, 2016b.
- Rusu, A. A., Vecerik, M., Rothörl, T., Heess, N., Pascanu, R., and Hadsell, R. Sim-to-real robot learning from pixels with progressive nets, 2018.
- Schulman, J., Moritz, P., Levine, S., Jordan, M., and Abbeel, P. High-dimensional continuous control using generalized advantage estimation, 2018.
- Schwarz, J., Luketina, J., Czarnecki, W. M., Grabska-Barwinska, A., Teh, Y. W., Pascanu, R., and Hadsell, R. Progress & compress: A scalable framework for continual learning, 2018.
- Silver, D., Hubert, T., Schrittwieser, J., Antonoglou, I., Lai, M., Guez, A., Lanctot, M., Sifre, L., Kumaran, D., Graepel, T., Lillicrap, T., Simonyan, K., and Hassabis, D. A general reinforcement learning algorithm that masters chess, shogi, and go through self-play. *Science*, 362 (6419):1140–1144, 2018. doi: 10.1126/science.aar6404. URL <https://www.science.org/doi/abs/10.1126/science.aar6404>.
- Spiteri, K., Uргаonkar, R., and Sitaraman, R. K. Bola: Near-optimal bitrate adaptation for online videos. *IEEE/ACM Transactions on Networking*, 28(4):1698–1711, 2020.
- Sun, Y., Yin, X., Jiang, J., Sekar, V., Lin, F., Wang, N., Liu, T., and Sinopoli, B. Cs2p: Improving video bitrate selection and adaptation with data-driven throughput prediction. In *Proceedings of the 2016 ACM SIGCOMM Conference, SIGCOMM '16*, pp. 272–285, New York, NY, USA, 2016. Association for Computing Machinery. ISBN 9781450341936. doi: 10.1145/2934872.2934898. URL <https://doi.org/10.1145/2934872.2934898>.
- Sutton, R. S. and Barto, A. G. *Reinforcement Learning: An Introduction*. A Bradford Book, Cambridge, MA, USA, 2018. ISBN 0262039249.
- Taylor, M. E. and Stone, P. An introduction to intertask transfer for reinforcement learning. *AI Magazine*, 32 (1):15, Mar. 2011. doi: 10.1609/aimag.v32i1.2329. URL <https://ojs.aaai.org/index.php/aimagazine/article/view/2329>.
- Thomas, P. S. *Safe reinforcement learning*. PhD thesis, University of Massachusetts Libraries, 2015.
- Uhlenbeck, G. E. and Ornstein, L. S. On the theory of the brownian motion. *Phys. Rev.*, 36:823–841, Sep 1930. doi: 10.1103/PhysRev.36.823. URL <https://link.aps.org/doi/10.1103/PhysRev.36.823>.
- van Hasselt, H., Guez, A., Hessel, M., Mnih, V., and Silver, D. Learning values across many orders of magnitude, 2016.
- Williams, R. J. and Peng, J. Function optimization using connectionist reinforcement learning algorithms. *Connection Science*, 3(3):241–268, 1991.
- Yan, F. Y., Ayers, H., Zhu, C., Fouladi, S., Hong, J., Zhang, K., Levis, P., and Winstein, K. Learning in situ: a randomized experiment in video streaming. In *17th {USENIX} Symposium on Networked Systems Design and Implementation ({NSDI} 20)*, pp. 495–511, 2020.
- Yin, X., Jindal, A., Sekar, V., and Sinopoli, B. A control-theoretic approach for dynamic adaptive video streaming over http. In *Proceedings of the 2015 ACM Conference on Special Interest Group on Data Communication*, pp. 325–338, 2015.

Zaheer, M., Kottur, S., Ravanbakhsh, S., Póczos, B.,  
Salakhutdinov, R., and Smola, A. Deep sets, 2018.

## A RL ALGORITHMS

### A.1 A2C

The main idea in A2C is to calculate the gradient of the expected returns with respect to a policy  $\pi_\theta$ , characterized by parameters  $\theta$  and based on sampled interactions using  $\pi_\theta$ .

$$\nabla_\theta \mathbb{E}_{\pi_\theta} \left[ \sum_{t=0}^H \gamma^t r_t \right] = \mathbb{E}_{\pi_\theta} \left[ \nabla_\theta \log \pi(s_t, a_t; \theta) R_t \right]$$

$R_t$  (return in state  $s_t$ ) is a high-variance random variable. To decrease the variance and improve training speed and stability, a baseline can be deducted from the return, without biasing the gradient. The used baseline is the expected return when using  $\pi_\theta$  ( $V_{\pi_\theta}(s_t) = \mathbb{E}_{\pi_\theta}[R_t]$ ), and the result of decreasing this baseline is called the advantage. Finally, using stochastic gradient ascent we have:

$$\theta \leftarrow \theta + \alpha_\pi \mathbb{E}_{\pi_\theta} \left[ \nabla_\theta \log \pi(s_t, a_t; \theta) (R_t - V_{\pi_\theta}(s_t)) \right]$$

We further improve the variance of A2C by employing Generalized Advantage Estimation (GAE) (Schulman et al., 2018). We also use entropy regulation (Williams & Peng, 1991; Mnih et al., 2016) to incentivize exploration during training. The entropy term decays from an initial value to zero (full exploitation), as non-zero values lead to sub-optimal policies (Ahmed et al., 2019). To estimate the expected return, we can train a separate critic with parameters  $\phi$  using mean squared error loss and returns as targets:

$$\phi \leftarrow \phi - \alpha_v \mathbb{E}_{\pi_\theta} \left[ \nabla_\phi (V^{\pi_\theta}(s_t; \phi) - R_t)^2 \right]$$

### A.2 DQN

The optimal Q-value  $Q^*(s_t, a_t)$  is the value of picking action  $a_t$  in state  $s_t$ , when all subsequent actions come from an optimal policy. We can learn  $Q^*$  by repeatedly applying the optimal Bellman operator to any starting estimate:

$$Q^*(s_t, a_t) = r(s_t, a_t) + \gamma \max_{a_{t+1} \in \mathcal{A}} [Q^*(s_{t+1}, a_{t+1})]$$

This operator holds, regardless of what policy created the sample. Also note that the optimal policy is the action with the highest Q-value, also known as the greedy policy. So DQN's training procedure starts by picking random actions and using the samples to train a Q-network. As training goes forward and the Q-network's estimates of the optimal Q-values are more precise, we gradually shift the policy from random to optimal.

We use Double Deep Q Network (DDQN) in this paper, which uses the same principle as DQN but uses techniques to reduce overestimation and improve stability (Hasselt et al., 2016). We also apply soft target network updates (also known as Polyak averaging) to increase stability (Lillicrap et al., 2019).

## B STRAGGLER MITIGATION

### B.1 Workloads

We have a trace from a production web framework cluster at AnonCo, collected from a single day in February 2018. The framework processes high-level web requests and breaks them down into subrequests that are issued to various backend services (e.g., to get product details, recommended items, billing information, etc.). These traces exhibit substantial variance, both in short durations and in longer ones. We use several of the traces from the different backend services as workloads in our straggler mitigation experiments:

- **Picasso** from *picassoPageObjectServiceV8*; a full-day trace. Used in evaluating offline training.
- **OneStore** from *oneStoreRecommendationService*; a full-day trace. Used in evaluating offline training.
- **Marketplace** from *Marketplace Collections/Entitlements Service*; a full-day trace. Used in evaluating offline training.
- **Workload A** from *TreatmentAssignmentService*; a 1-hour trace. Used in experiments with non-stationarity.
- **Workload B** from *Marketplace Collections/Entitlements Service*; a 1-hour trace. Used in experiments with non-stationarity.
- **Workload C** from *Marketplace Catalog*; a 1-hour trace. Used in experiments with non-stationarity.

These workloads are visualized in Figure 15 and Figure 17. Shaded lines denote each attribute of a workload, namely job sizes and arrival rates, in 5 second time windows. Solid color lines are Exponentially Weighted Moving Averages of the shaded lines.

### B.2 Extended results

#### B.2.1 Offline training

We described in §4 why offline training is not well-suited to non-stationary environments. Here we provide conclusive evidence for it. We train an RL agent using a training workload and the on-policy A2C algorithm. We deploy the final policy to an environment with a test workload.

Train and test workloads are chosen from three day-long traces (*Marketplace Collections*, *OneStore* and *Picasso*), as depicted in Figure 17.

Figure 13 visualizes the performance of a model based on its train/test workload. This heatmap normalizes the average tail latency with the performance of a no-hedging agent, and the agent with matching train/test workloads. Note

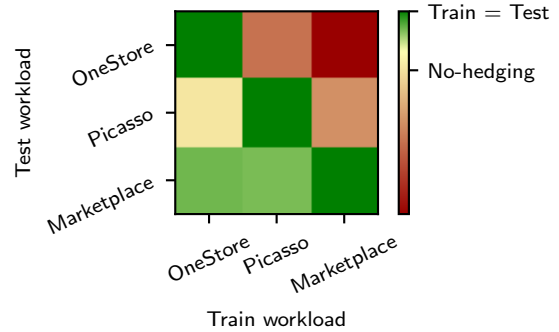


Figure 13. Average tail latency when testing offline-trained models on different workloads. Offline models’ test performance degrades if the workload differs from the training workload, with stronger degradation for more dissimilar workloads.

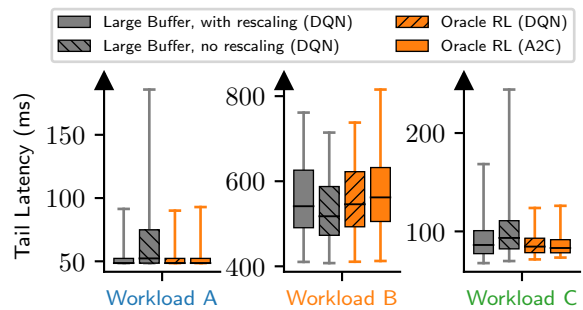


Figure 14. Tail latency distribution after convergence in Scenario I, when  $T_{sw} = T_c$  (similar to Figure 6). Without considering rewards scales, DQN favors workloads with high magnitude rewards at the expense of others.

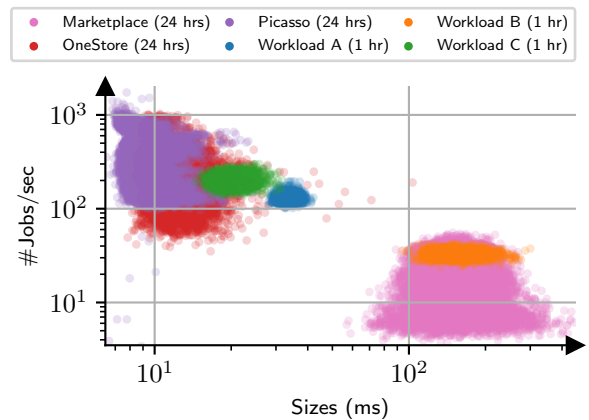


Figure 15. Arrival rates and sizes, for six workloads from five traces (*Workload B* is from the *Marketplace* trace). Each point shows five-second averages. Note the  $\log_{10}$  scale on both axes.

the clear degradation in performance when the test/train workloads do not match, even for similar workloads such as *OneStore* and *Picasso*. Offline training, even under the favourable conditions of a perfect simulator and stable on-policy training is not viable.



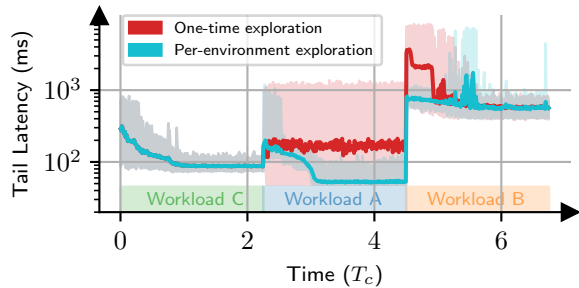


Figure 16. Tail latency across time, when we start with workload C. Shaded regions denote min-to-max of tail latency across 3 random seeds. Each workload is given enough time to converge ( $T_{sw} = 2.25T_c$ ).

### B.2.2 Per-environment exploration

Figure 16 demonstrates the effect of exploring once for each workload. This plot shows the tail latency over the course of the experiment. We see that while one-time exploration (for  $T_c$  time) fails to handle new workloads (e.g., Workload A), per-environment exploration converges to a good policy for each workload. One-time exploration is clearly not a viable approach.

### B.2.3 DQN scaling

A further nuance with the off-policy approach, is reward scaling. Since the Q-value network will train on samples from multiple workloads with different magnitudes (latency in one workload can be  $10\text{ ms}$  while  $500\text{ ms}$  in another), workloads with larger rewards will be overemphasized in the L2 loss in training. Therefore, the rewards must be normalized but done so consistently. Figure 14 shows the effect; If scaling is not performed, workloads with smaller rewards (latencies), such as workloads A and C are sacrificed for superior performance in workloads with large rewards. Besides manual normalization, methods exist for automatic adaptation to reward scales (van Hasselt et al., 2016; Hessel et al., 2018).

## B.3 Training and environment setup

Our implementations of A2C and DQN use the Pytorch (Paszke et al., 2019) library. Table 2 is a comprehensive list of all hyperparameters used in training and the environment.

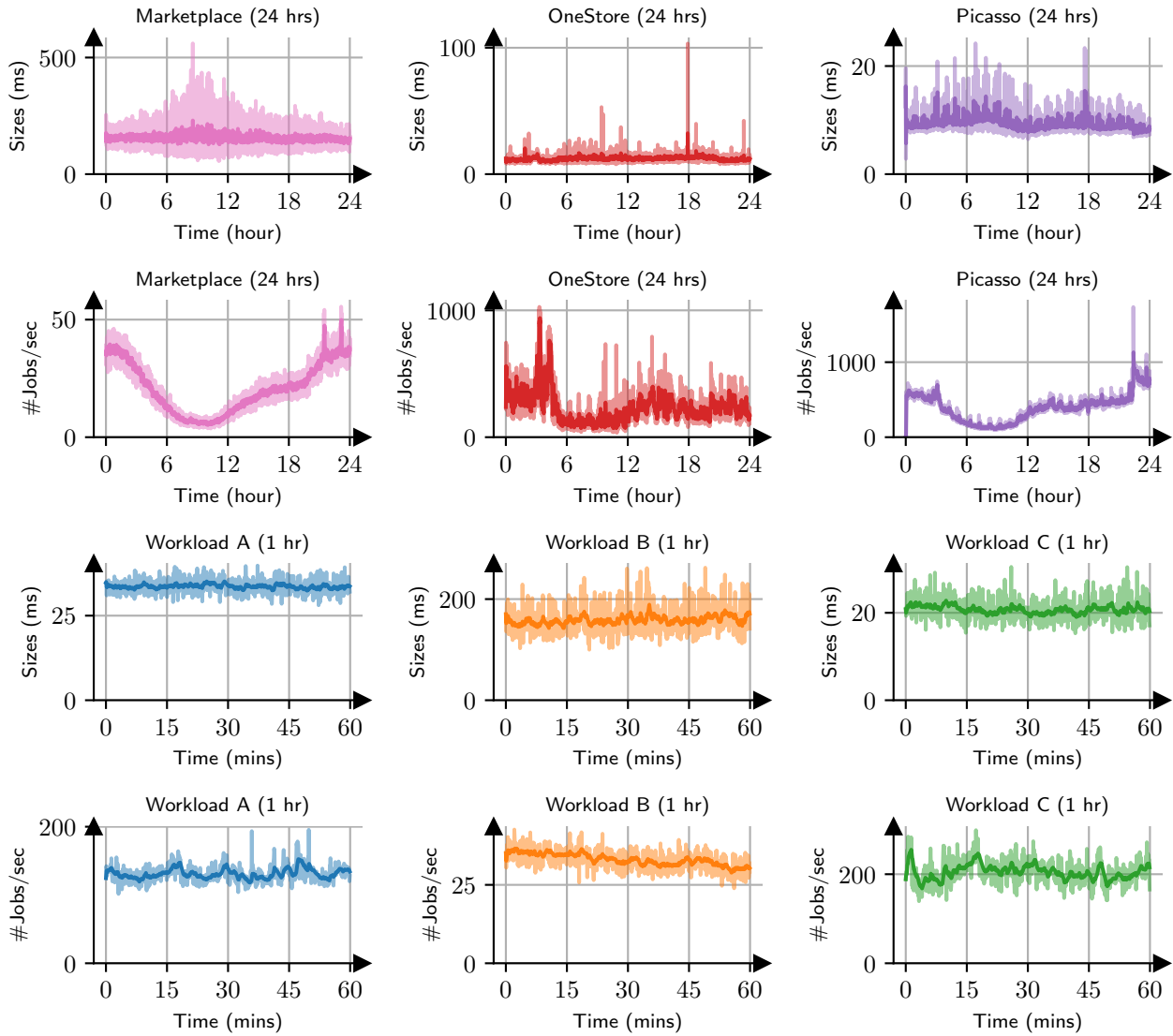


Figure 17. Visual depiction of workloads through time.

Group	Hyperparameter	Value
Neural network	Hidden layers	$\phi$ network: (16, 8)
		$\rho$ network: (16, 8)
	Hidden layer activation function	Relu
	Output layer activation function	A2C actor: Softmax
		A2C critic: Identity mapping
		DQN: Identity mapping
	Optimizer	Adam (Kingma & Ba, 2017)
	Learning rate	0.001
	$\beta_1$	0.9
	$\beta_2$	0.999
	$\epsilon$	$10^{-8}$
Weight decay	$10^{-4}$	
RL training (general)	Episode lengths	128
	Epochs to convergence ( $T_c$ )	6000 (728000 samples)
	Random seeds	3
	$\gamma$	0.9
A2C training	Entropy schedule	0.1 to 0 in 5000 epochs
	$\lambda$ (for GAE)	0.95
DQN training	Initial fully random period	1000 epochs
	$\epsilon$ -greedy schedule	1 to 0 in 5000 epochs
	Polyak $\alpha$	0.01
	Buffer size in Last $N$	$10^6$
	Buffer size in Long-term short-term	$10^6$ (short)
	Buffer size in Multipler buffers	$10^6$ for each
Environment	Number of servers $n$	10
	Number of actions	7
	Timeouts of actions (millisecs)	{3,10,30,60,100,300, $\infty$ (no-hedging)}
	Action time window	500 ms
	(Slow down rate $k$ , probability $p$ )	(10, 10%)
	Observation workload aggregation steps ( $m$ )	4
	Safe guard unsafety upper limit	50 jobs
	Safe guard return to safety lower limit	3 jobs

Table 2. Training setup and hyperparameters for straggler mitigation experiments.

## C ADAPTIVE BIT RATE

### C.1 User Groups

To create various bandwidth distributions for our experiments, we use a generative process. This process was designed to cover three important characteristics in bandwidth traces: **(a)** The average bandwidth the whole distribution observes. This represents how fast the users’ networks are in total. **(b)** The variation in average bandwidth among users. This represents how similar or different networks of a group’s users are. **(c)** The variation in the bandwidth trace for each user. This represents how stable a user’s network is at providing bandwidth.

The user groups we generate provide a good coverage over these three characteristics:

- **User group 1** is a low bandwidth group, with medium diversity among users and high variance in each user trace.
- **User group 2** is a high bandwidth group, with high diversity among users and low variance in each user trace.
- **User group 3** is a medium bandwidth group, with low diversity among users and medium variance in each user trace.
- **User group 4** is a medium to low bandwidth group, with low diversity among users and medium variance in each user trace.
- **User group 5** is a medium bandwidth group, with very high diversity among users and high variance in each user trace.

Sample traces for these groups can be observed at Figure 19.

The generative process is a mixture of a Markov chain and an Ornstein–Uhlenbeck process (Uhlenbeck & Ornstein, 1930). The Markov chain generates a coarse bandwidth trace, which prior work shows is an appropriate model for TCP throughput (Sun et al., 2016). The Ornstein–Uhlenbeck process, which is a mean-reverting variant of Brownian motion adds a random walk to the coarse output of the Markov chain. Contrary to previous work (Akhtar et al., 2018), we use a mean reverting random walk instead of i.i.d. Gaussian noise to model smooth changes in throughput as well. We use a uniform initial distribution for the Markov chain. Overall, the degrees of freedom in this process are: **(a)** the state space of the Markov chain, **(b)** the transition kernel of the Markov chain, **(c)** the scale and dissipation rate of the Ornstein–Uhlenbeck process.

### C.2 Extended results: QoE breakdown

Recall that QoE is a combination of several conflicting objectives. Namely, the quality of streaming, the smoothness

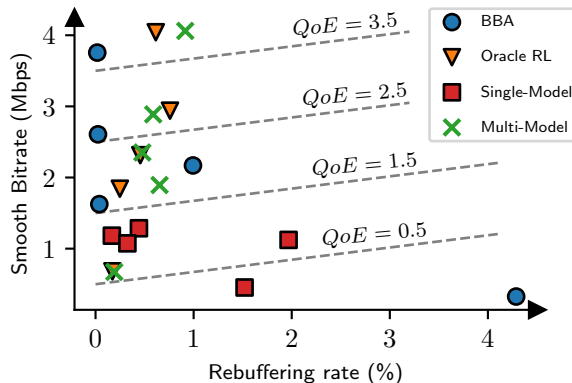


Figure 18. Break down of QoE in Figure 12; smooth bitrate refers to the chosen bitrate subtracted by the smoothness penalty.

of that quality across chunks and rebuffering:

$$QoE_t = q_t - |q_t - q_{t-1}| - \mu \cdot \max(0, \frac{S_t}{c_t} - b_t)$$

To interpret the QoE results in Figure 12, we visualize the smoothed bitrate of choices against rebuffering. Smoothed bitrate is the combination of the first two terms in the QoE. Figure 18 demonstrates this breaks down. BBA avoids rebuffering when bandwidth is stable at the cost of lower quality, but in variable bandwidths it repeats the same mistake of underestimating the risk of rebuffering. Single expert policies are confused by the non-stationary nature of the problem and break down in all cases. Multiple experts manage to avoid the confusion and CF by design and adapt to any bandwidth distribution.

### C.3 Training setup

Similar to the straggler mitigation experiments, our implementation of A2C uses the Pytorch (Paszke et al., 2019) library. We use the ABR implementation in (Mao et al., 2019a) for our experiments. Table 3 is a comprehensive list of all hyperparameters used in training and the environment. For the video in the ABR streaming, we use “Envivio-Dash3” from the DASH-246 JavaScript reference client (DASH Industry Form, 2016).

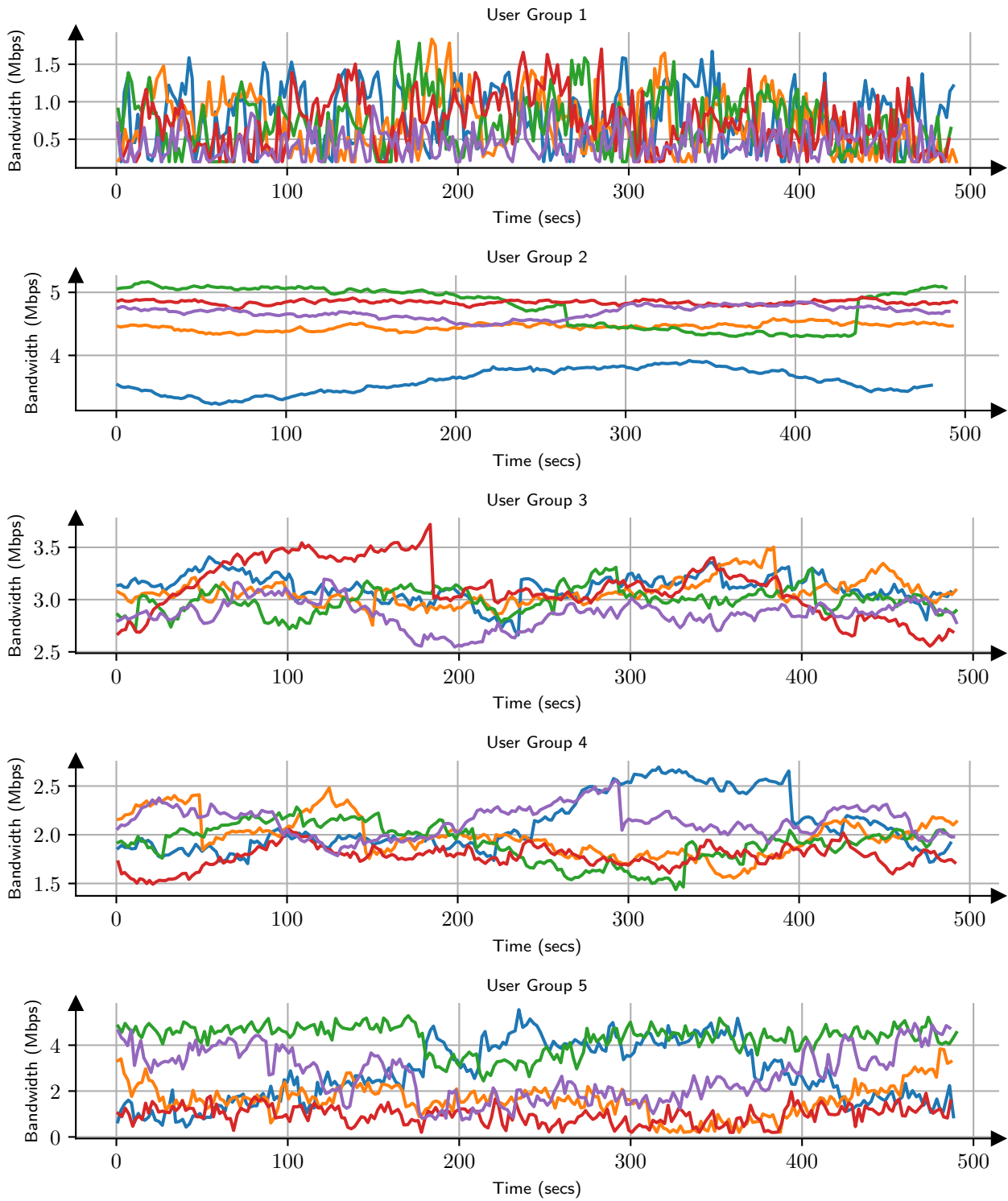


Figure 19. Visual depiction of user group bandwidths through time. Each plot has 5 samples.

Group	Hyperparameter	Value
Neural network	Hidden layers	(64, 32)
	Hidden layer activation function	Relu
	Output layer activation function	A2C actor: Softmax
		A2C critic: Identity mapping
	Optimizer	Adam (Kingma & Ba, 2017)
	Learning rate	0.001
	$\beta_1$	0.9
	$\beta_2$	0.999
	$\epsilon$	$10^{-8}$
	Weight decay	$10^{-4}$
A2C training	Episode lengths	490
	Epochs to convergence ( $T_c$ )	3000 (1470000 samples)
	Random seeds	3
	$\gamma$	0.96
	Entropy schedule	0.25 to 0 in 2000 epochs
	$\lambda$ (for GAE)	0.95
Environment	Chunk length $T$	4
	Number of actions (bitrates)	6
	Fake-Replay starting threshold	$\min(20, 99^{\text{th}}$ of first 5 episode buffers)
	Fake-Replay schedule	From start to 0 in 2000 epochs
BBA	Reservoir	5 seconds (as in (Mao et al., 2017))
	Cushion	10 seconds (as in (Mao et al., 2017))

Table 3. Training setup and hyperparameters for ABR experiments.